Inorganic Chemistry

Article

pubs.acs.org/IC

Incorporation of Cu^{2+} Ions into Nanotubular Uranyl Diphosphonates

Pius O. Adelani,[†] Nathaniel D. Cook,[†] Jean-Marie Babo,[†] and Peter C. Burns*[,†,‡]

[†]Department of Civil and Environmental Engineering and Earth Sciences and [‡]Department of Chemistry and Biochemistry, University of Notre Dame, Notre Dame, Indiana 46556, United States

Supporting Information

ABSTRACT: Three new multidimensional polymetallic uranyl diphosphonates were crystallized under mild hydrothermal conditions: $[Cu(H_2O)]_2\{(UO_2)_4F_2[(PO_3C_6H_4)(C_6H_4PO_3H)_3]_2(bipym)\}\cdot 6H_2O$ (**1**), $[Cu(H_2O)]_2\{(UO_2)_4[(C_6H_4PO_3)(C_6H_4PO_3H)]_4(bipym)\}$ (**2**), and $Cu\{(UO_2)(C_6H_4PO_3)_2(bipym)\}\cdot H_2O$ (**3**). Compound **1** consists of UO_6F pentagonal bipyramids connected by diphosphonate moieties into a tubular channel. The Cu^{2+} cations are stabilized between the nanotubular subunits by 2,2′-bipyrimidine (bipym). The structure of **2** is similar to **1**, except that it consists of relatively rare UO_6 tetragonal bipyramids bridged by diphosphonate groups. Compound **3** also contains UO_6 tetragonal bipyramids. Unlike compounds **1** and **2**, only two of the tetradentate N atoms of the binucleating bipym group are coordinated. All three compounds show luminescent properties under ambient conditions, with evidence of the characteristic vibronically coupled charge-transfer based uranyl cation emissions.

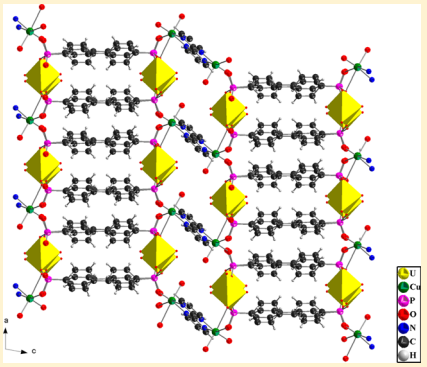

INTRODUCTION

The development of new synthetic strategies for the design of heterometallic uranyl-organic coordination polymers is a key target in modern actinide coordination chemistry.[1] The intense interest in these complexes is due to not only their intriguing structural diversity, but also their potential in various chemical applications, such as photochemistry,[1−4] gas sorption,[1f,g] ion-exchange,[5] intercalation chemistry,[6] ionic conductivity,[7] nonlinear optics,[8] magnetic interactions,[9] etc. One of the most common strategies employed in constructing bimetallic uranyl-organic complexes is based on the use of multifunctional ligands to incorporate the second metal center, such as carboxyphosphonates.[1] The presence of the bifunctional group allows for the preferential binding of the harder metal center by the harder functionality and vice versa. Another approach involves the use of the chelating ligands.[2] However, other conditions, such as the use of second metal centers with appropriate size and geometry, make this option considerably more challenging and serendipitous results are more common than predictable outcomes. Recent work by Zhong-Ming Sun and his team have delineated the necessity of using a bimetallic uranyl salt, $Zn(UO_2)(OAc)_4\cdot 7H_2O$, as a reagent in the formation of bimetallic uranyl diphosphonate complexes.[3] The use of N-donor secondary linkers is another attractive alternative in which the second metal center (i.e., transition metals) is stabilized by an N-donor ligand.[4] Among other strategies, the logical design of bifunctional ligands and an appropriate choice of auxiliary ligands are the most attractive strategies that have been adequately investigated in the literature.[1,4]

Recent investigations in our laboratory and among other groups have examined the bifunctional ligand approach to design heterobimetallic uranyl carboxyphosphonates.[1] The disparity in steric influence from the carboxyphenylphosphonates and phosphonoacetates vastly expands the topologies of the materials yielded.[1] We obtained a three-dimensional uranyl-copper(II) coordination polymer with 1,3-carboxyphenylphosphonate, and passivated the extension along the third axis by using 1,2-carboxyphenylphosphonate to obtain lower-dimensional complexes.[1b,c] Unlike the phosphonoacetate system that accommodates a series of transition-metal and lanthanide cations,[1a,e−i] we incorporated a variety of transition metals in the 1,2-carboxyphenylphosphonate system.[1b,c] The second most promising approach involves the use of N-donor linkers such as 2,2′-bipyridine, 1,10-phenanthroline, 1H-benzo[d]imidazole, and 1-phenyl-1H-imidazole.[4] Unfortunately, the phenyl rings from the auxiliary ligands terminate the surface of the polymers and truncate the dimensionality of the bimetallic complexes.[4] A binucleating tetradentate ligand with nitrogen-donor atoms such as 2,2′-bipyrimidine (bipym) has been employed recently to chelate the second metal center without truncating the surfaces.[10]

We have demonstrated that the use of diphosphonate ligands with rigid phenyl spacers allows for the synthesis of multidimensional layered uranyl coordination polymers that are rigidly pillared by diphosphonates.[11] The structural topologies and complexities of these materials are further enhanced through the incorporation of structure-directing agents.[1d,5a,b,11a,b,d−f] Herein, we report the synthesis, structural characterization, and spectroscopic properties of three multidimensional copper(II) uranyl diphosphonate complexes, including bipym as secondary linkers.

Received: January 28, 2014
Published: April 4, 2014

   dx.doi.org/10.1021/ic500220d | *Inorg. Chem.* 2014, 53, 4169−4176

EXPERIMENTAL SECTION

Synthesis. $UO_2(NO_3)_2{\cdot}6H_2O$ (98%, International Bio-Analytical Industries), $UO_2(C_2H_3O_2)_2{\cdot}2H_2O$ (98%, Alfa-Aesar), $CuCl_2{\cdot}2H_2O$ (99%, Aldrich), HF (48 wt %, Aldrich), 4,4′-biphenylenebisphosphonic acid (98%, Epsilon Chimie), and 2,2′-bipyrimidine (95%, Aldrich) were used as received. Reactants were combined in Teflon-lined steel autoclaves with a volume of 23 mL. The water used in all reactions was distilled and Millipore-filtered, and had a resistance of 18.2° MΩ cm. ***Caution!*** *Uranium is radioactive and studies such as those described here should only be conducted in appropriate facilities by personnel trained in the safe handling of radioactive materials.*

Table 1. Crystallographic Data for $[Cu(H_2O)]_2\{(UO_2)_4F_2[(PO_3C_6H_4)(C_6H_4PO_3H)_3]_2(bipym)\}{\cdot}6H_2O$ (1), $[Cu(H_2O)]_2\{(UO_2)_4[(C_6H_4PO_3)(C_6H_4PO_3H)]_4(bipym)\}$ (2), and $Cu\{(UO_2)(C_6H_4PO_3)_2(bipym)\}{\cdot}H_2O$ (3)

	1	2	3
formula mass	1385.93	1318.93	817.86
color and habit	green, tablet	green, tablet	green, needle-like
space group	$P2_1/c$ (No. 14)	$P\bar{1}$ (No. 2)	$P\bar{1}$ (No. 2)
a (Å)	18.608(3)	9.2355(18)	9.053(3)
b (Å)	9.9149(14)	11.278(2)	10.786(3)
c (Å)	19.979(3)	18.640(4)	13.549(4)
α (deg)	90	93.948(2)	81.354(4)
β (deg)	93.926(2)	98.273(2)	74.852(3)
γ (deg)	90	109.090(2)	68.034(3)
V (Å)	3677.5(9)	1801.6(6)	1182.3(6)
Z	4	2	2
T (K)	100	100	100
λ (Å)	0.71073	0.71073	0.71073
ρ_{calcd} (g cm^{-3})	2.503	2.431	2.297
μ (Mo Kα) (mm^{-1})	9.626	9.807	7.935
$R(F)$ for $F_0^2 > 2\sigma(F_0^2)^a$	0.046	0.037	0.047
$Rw(F_0^2)^b$	0.122	0.085	0.116

$^aR(F) = \sum||F_0| - |F_c||/\sum|F_0|$. $^bR(F_0^2) = [\sum w(F_0^2 - F_c^2)^2/\sum w(F_0^4)]^{1/2}$.

[Cu(H$_2$O)]$_2${(UO$_2$)$_4$F$_2$[(PO$_3$C$_6$H$_4$)(C$_6$H$_4$PO$_3$H)$_3$]$_2$(bipym)}·6H$_2$O ***(1)***. $UO_2(NO_3)_2{\cdot}6H_2O$ (50.2 mg, 0.1 mmol), $CuCl_2{\cdot}2H_2O$ (17.1 mg, 0.1 mmol), 4,4′-biphenylenebisphosphonic acid (31.8 mg, 0.1 mmol), 2,2′-bipyrimidine (15.8 mg, 0.1 mmol), 1.0 mL of water, and HF (~15 μL) were placed in a 23-mL autoclave that was subsequently sealed. It was placed in a box furnace at 160 °C for 5 days, followed by slow cooling at 9 °C/h to ambient conditions. The product was recovered by filtration and washed with methanol and distilled water, and then was allowed to dry in air. Green block-shaped crystals of **1** were recovered, together with a fine-grained precipitate. The fine-grained precipitate was the major product, whereas crystals of **1** corresponded to 40% of the products.

[Cu(H$_2$O)]$_2${(UO$_2$)$_4$[(C$_6$H$_4$PO$_3$)(C$_6$H$_4$PO$_3$H)]$_4$(bipym)} ***(2)*** *and Cu{(UO$_2$)(C$_6$H$_4$PO$_3$)$_2$(bipym)}·H$_2$O* ***(3)***. Substitution of $UO_2(C_2H_3O_2)_2{\cdot}2H_2O$ (42.4 mg, 0.1 mmol) for the uranyl nitrate in the reaction procedure for **1** resulted in the isolation of green block-shaped crystals of **2** and powder products. (Note: **2** comprised about 40% of the products.) Green needlelike crystals of **3** and powder products were isolated when the amount of HF was increased to ~30 μL in either reaction **1** or **2**. Compound **3** was also identified as one of the phases in the reaction products containing **1** and **2** by powder X-ray diffraction (XRD).

Crystallographic Studies. Single-crystal X-ray diffraction data was collected for appropriate crystals of each compound

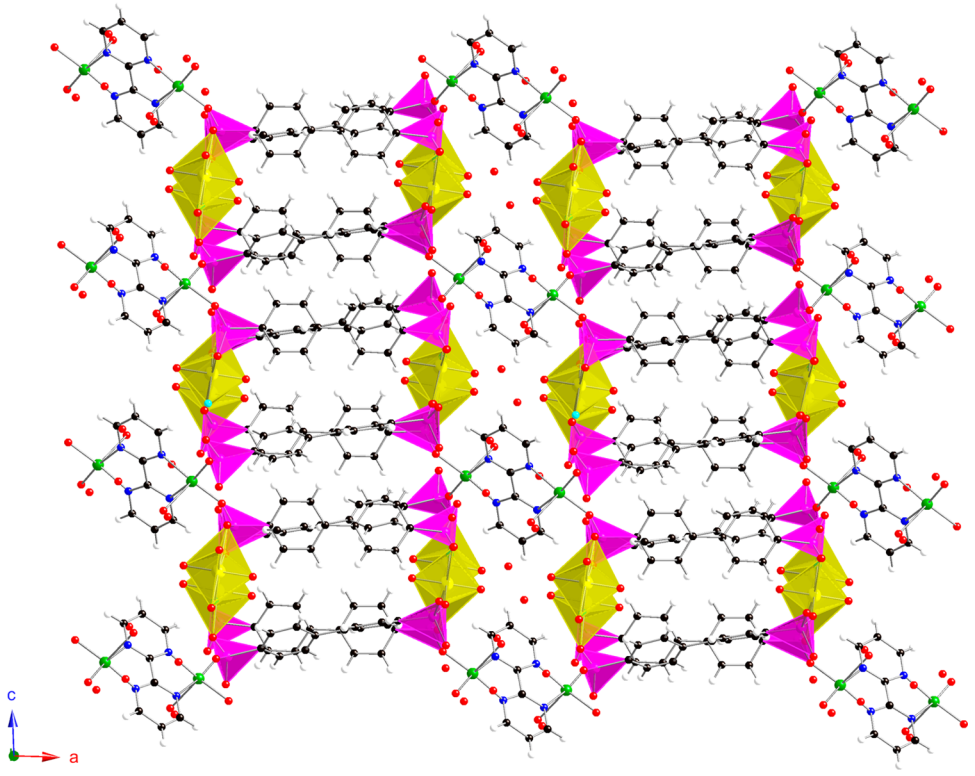

Figure 1. View down the [010] axis, showing the packing of the tubular uranyl diphosphonate units and the incorporated copper(II) cations including bipym in **1**. [Legend: UO_6F units = yellow, copper = green, phosphorus = magenta, fluorine = cyan, oxygen = red, nitrogen = blue, carbon = black, and hydrogen = white.]

dx.doi.org/10.1021/ic500220d | Inorg. Chem. 2014, 53, 4169−4176

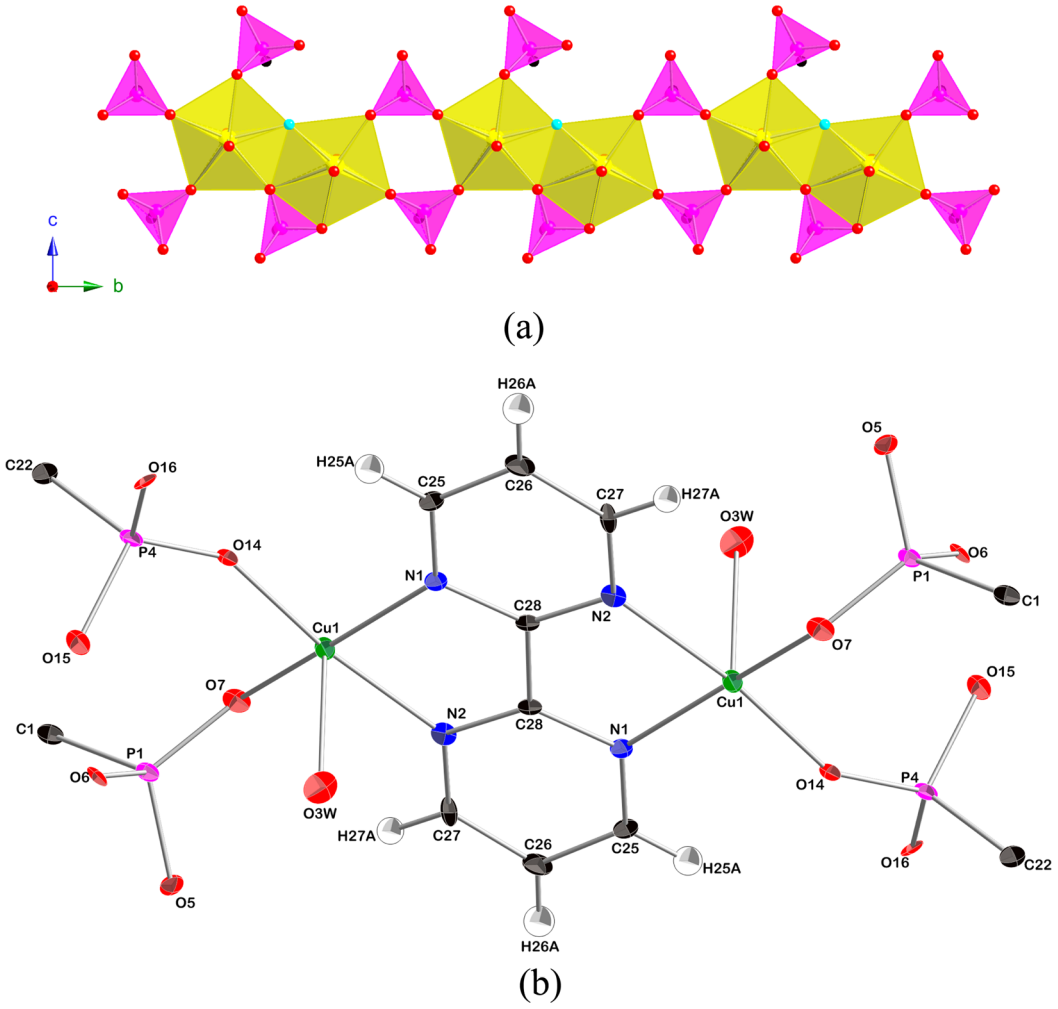

Figure 2. (a) A polyhedral representation of the uranyl-phosphonate chain in **1** viewed along the [100] axis, showing the edge-sharing UO_6F dimers that are linked by the phosphonate moiety. (b) A drawing of the local coordination environment around the square pyramidal copper(II) metal center in **1** and the sandwiched secondary linker, bipym. [Legend is the same as that given in the caption for Figure 1.]

using a Bruker APEXII Quazar CCD X-ray diffractometer with Mo Kα radiation produced by a IμS microfocus sealed tube and conditioned using Montel optics. Unit-cell determinations and data collections were handled with the Bruker software APEXII. Data were collected using ω scans with frame widths of 0.5°, with exposure times in the range of 10−30 s per frame, depending on the crystal size. The data was integrated and corrected for Lorentz, polarization, and background effects using SAINT, and were corrected for absorption using SADABS. The structures were solved and refined using the SHELXTL suite of computer programs.[12] H positions on C atoms were included using riding models. All atoms in the final refinement, excluding H, were treated anisotropically. Crystallographic parameters are provided in Table 1, as well as Tables S1−S3 in the Supporting Information.

Powder X-ray Diffraction (XRD). A powder XRD pattern for each of the reaction products was collected using an automated Bruker diffractometer in θ−θ configuration with a Lynxeye one-dimensional solid-state detector using Cu Kα radiation over the angular range of 5°−65° (2θ). The resulting patterns were compared with those calculated from the refined crystal structure models (see Figures S1 and S2 in the Supporting Information).

Spectroscopic Properties. Single crystals of each compound were used for the collection of fluorescence and absorption (250−1200 nm range) data using a Craic Technologies UV-vis-NIR microspectrophotometer with a fluorescence attachment under ambient conditions. Excitation for the fluorescence spectroscopy was achieved using 365-nm light from a Hg lamp (see Figures S3 and S4 in the Supporting Information). Infrared spectra for single crystals of **1**, **2**, and **3** were collected using a SensIR Technology IlluminatIR FT-IR microspectrometer. The spectra were collected with a diamond ATR objective.

RESULTS AND DISCUSSION

Synthesis. All the reagents used in all of the syntheses reported here were added in stoichiometrically equivalent quantities. The addition of HF to the reactants is essential; it serves as a mineralizing agent in all the syntheses as well as a ligand in **1**. Compounds **1** and **2** were synthesized by using uranyl nitrate and acetate, respectively, while **3** can be crystallized from either of these two reactions by increasing the amount of HF. The powder XRD patterns collected for the products of **1** and **2** indicate the presence of **3** in both reactions. The quantity of HF added to the reactants must be precisely controlled to prevent crystallization of uranium(IV) fluorides.

dx.doi.org/10.1021/ic500220d | Inorg. Chem. 2014, 53, 4169−4176

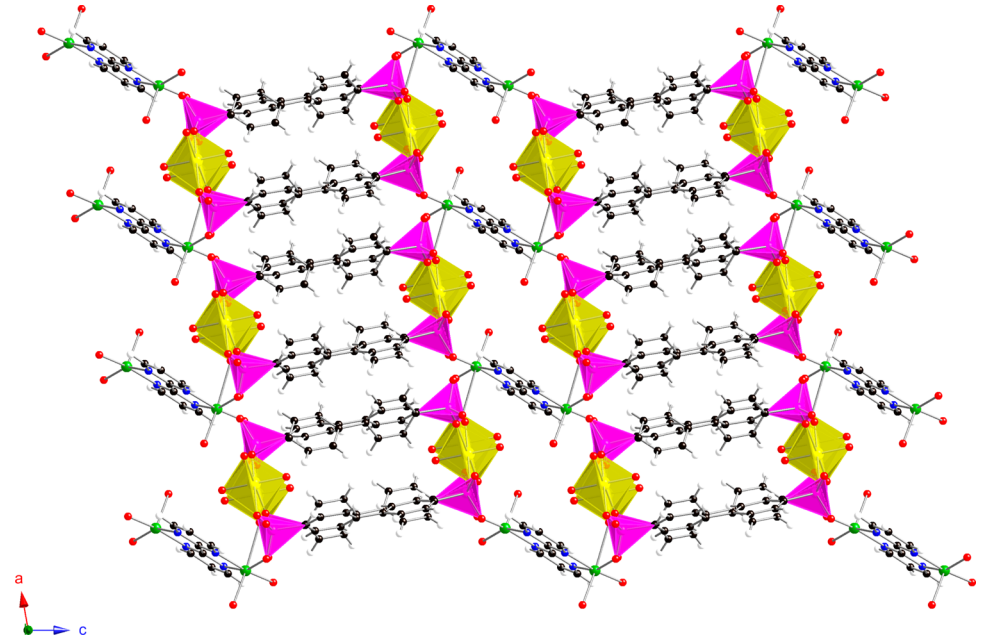

Figure 3. View down [010] showing the packing diagram of the tubular uranyl diphosphonate units and the incorporated copper(II) cations including 2,2′-bipyrimidine in **2**. [Legend: UO_6 units = yellow, copper = green, phosphorus = magenta, oxygen = red, nitrogen = blue, carbon = black, and hydrogen = white.]

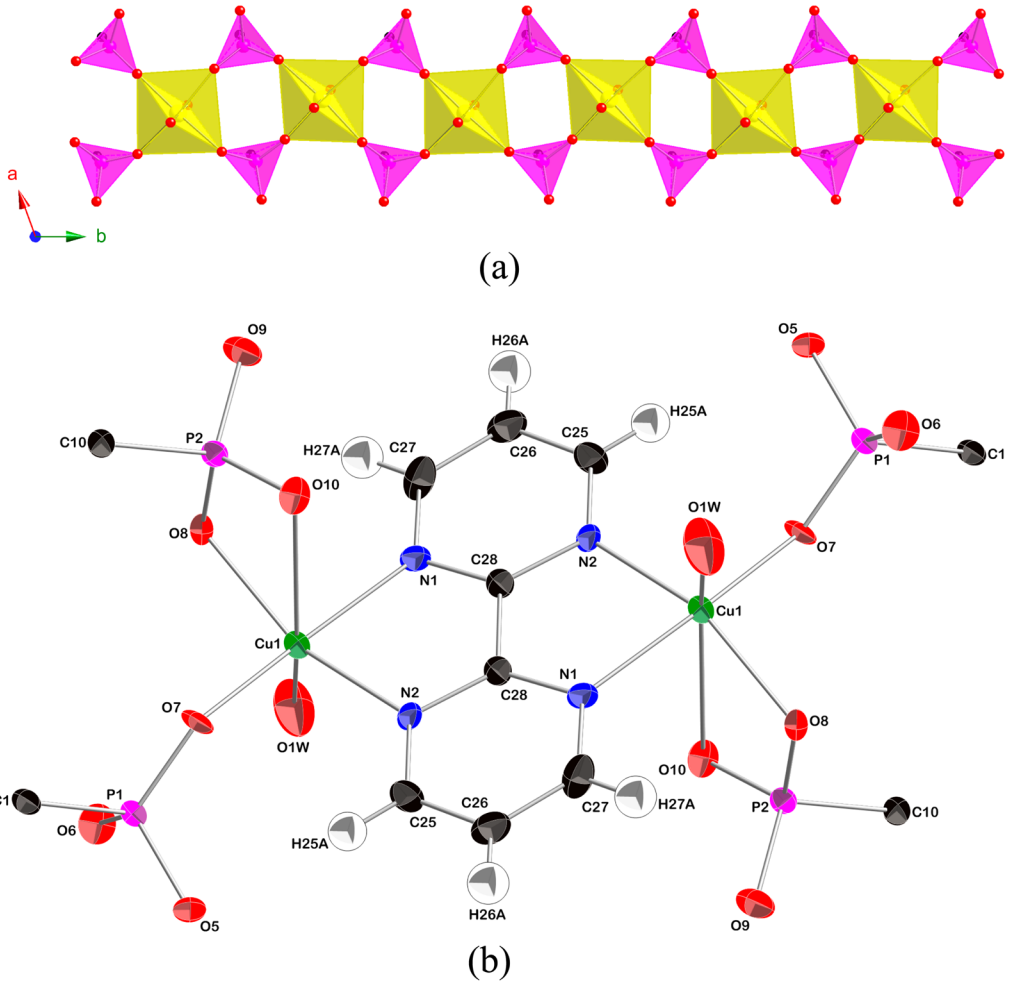

Figure 4. (a) A polyhedral view of **2** along the [001] axis, showing the monomeric UO_6 cations that are connected by the phosphonate moiety into chains. (b) A drawing of the local coordination environment around the distorted octahedral copper(II) metal center in **2** and the sandwiched secondary linker, bipym. Ellipsoids are shown in the 50% probability level. [Legend is the same as that given in the caption for Figure 3.]

dx.doi.org/10.1021/ic500220d | *Inorg. Chem.* 2014, 53, 4169−4176

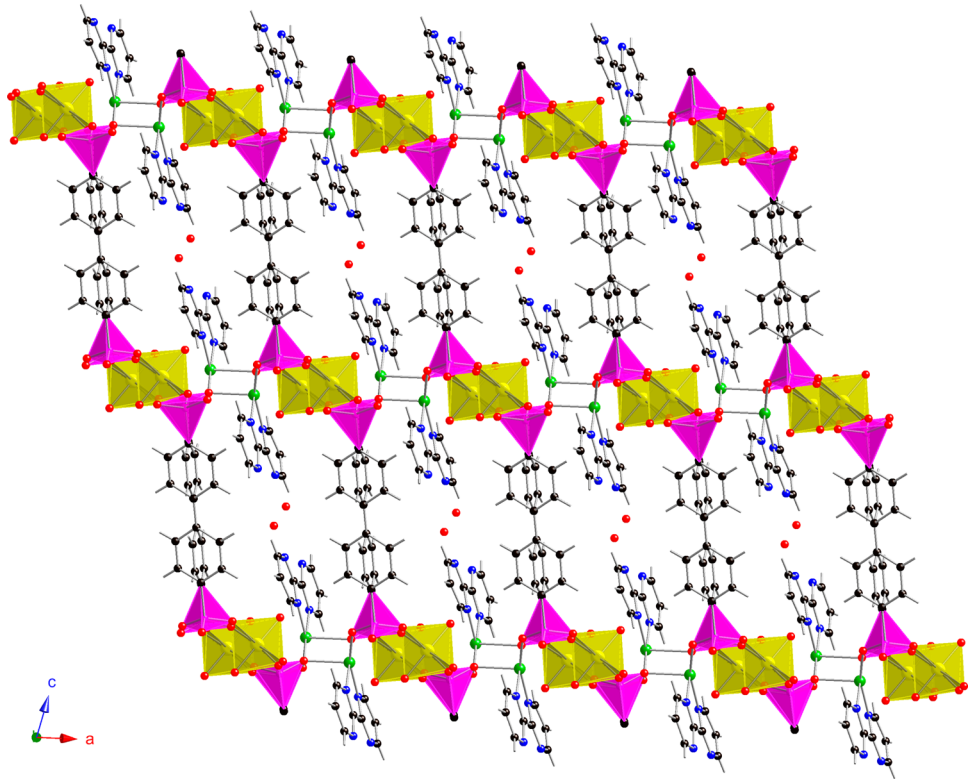

Figure 5. A view down the [010] axis, showing the packing diagram of the uranyl diphosphonate chains and the incorporated copper(II) cations including partially coordinated bipym in **3**. [Legend: UO_6 units = yellow, copper = green, phosphorus = magenta, oxygen = red, nitrogen = blue, carbon = black, and hydrogen = white.]

Structure of $[Cu(H_2O)]_2\{(UO_2)_4F_2[(PO_3C_6H_4)(C_6H_4PO_3H)_3]_2(bipym)\}\cdot 6H_2O$ (*1*). The overall structure of **1** consists of nanotubular uranyl diphosphonate subunits and Cu^{2+} ions that are stabilized between the tubes by bipym (see Figure 1). This compound is remarkable in that it incorporates the $[Cu_2(H_2O)_2(bipym)]^{4+}$ moiety without distorting the elliptical cross-section of the nanotubular topology or dimensions of the tubes.[5a] In contrast to the previously reported members of this family, $A_2\{(UO_2)_2F(PO_3HC_6H_4C_6H_4PO_3H)(PO_3HC_6H_4C_6H_4PO_3)\}\cdot 2H_2O$ (A = Cs^+ and Rb^+), the nanotubular structure is composed of edge-sharing dimers of uranyl polyhedra instead of the reported corner-sharing dimers of UO_6F pentagonal bipyramids (see Figure 2a).[5a] The shared edges are occupied by F and O atoms, thus the inclusion of HF is essential in the synthesis of **1**. Another key feature of this nanotubular structure is the presence of water molecules outside of the tubes, in contrast to earlier reported structures, where the tubes are filled with water molecules.[5a]

Two crystallographically unique uranium centers are present in this structure. Each is bonded to two oxo atoms that constitute the axial positions of UO_2^{2+} cations, with an average U═O bond distance of 1.763(6) Å. Four sites in the equatorial planes of the uranyl pentagonal bipyramids are oxygen atoms of the diphosphonate ligands, and U−O bond lengths range from 2.301(6) Å to 2.581(6) Å. The fifth equatorial site in each polyhedron is occupied by a F^- anion, with an average U−F bond distance of 2.310(5) Å. The calculated bond-valence sums for the uranyl cations are 5.97 and 5.96 valence units, which is consistent with the formal valence of U(VI).[13] The phosphonate moieties bound the uranyl cations and stabilize the dimers, and also provide linkages between the dimers to create chains extending along the [010] axis. Two crystallographically distinct phosphonate moieties are present in this structure:; the P−O bond lengths range from 1.498(7) to 1.589(6) Å. The longer P−O bond lengths are due to protonation of the terminal P−O groups. The Cu center is surrounded by a distorted five-coordinate CuN_2O_3 (4 + 1) square pyramid. Two oxygen atoms from PO_3 moieties and one chelating bipym form the equatorial plane of the pyramid, whereas the axial position is occupied by a weakly coordinated water molecule. The equatorial Cu−O bond distances are 1.892(6) Å and 1.930(6) Å, and the Cu−N bond distances are 2.013(8) Å and 2.039(8) Å, all of which are in agreement with literature values.[14] The axial $Cu-O_{water}$ bond distance of 2.487(6) Å is significantly longer than the equatorial bonds but remains within the values found for coordinated water molecules.[14] The calculated bond valence sum for the Cu(1) center is 1.83 valence units, which is in agreement with the Cu(II) oxidation state.[13]

Structure of $[Cu(H_2O)]_2\{(UO_2)_4[(C_6H_4PO_3)(C_6H_4PO_3H)]_4(bipym)\}$ (*2*). Despite the general nanotubular character of the structure of **2**, the coordination environments of the constituent UO_2^{2+}/Cu^{2+} cations are distinct from **1**. The overall structure contains two uranyl cations with similar coordination environments, two crystallographically unique phosphonate ligands, and one Cu(II) center with a co-crystallized water molecule (Figure 3). The nanotubular subunit is composed of monomeric UO_6 tetragonal bipyramids. The uranyl cations are bridged by PO_3 moieties to create a one-dimensional chain extending along the length of the nanotubular structure (see Figure 4a). In contrast to compound **1**, the polyhedral representation of the overall structure along [010] reveals a slightly slanted $[Cu_2(H_2O)_2(bipym)]^{4+}$ subunit relative to the orientation of the nanotubular subunits.

dx.doi.org/10.1021/ic500220d | *Inorg. Chem.* 2014, 53, 4169−4176

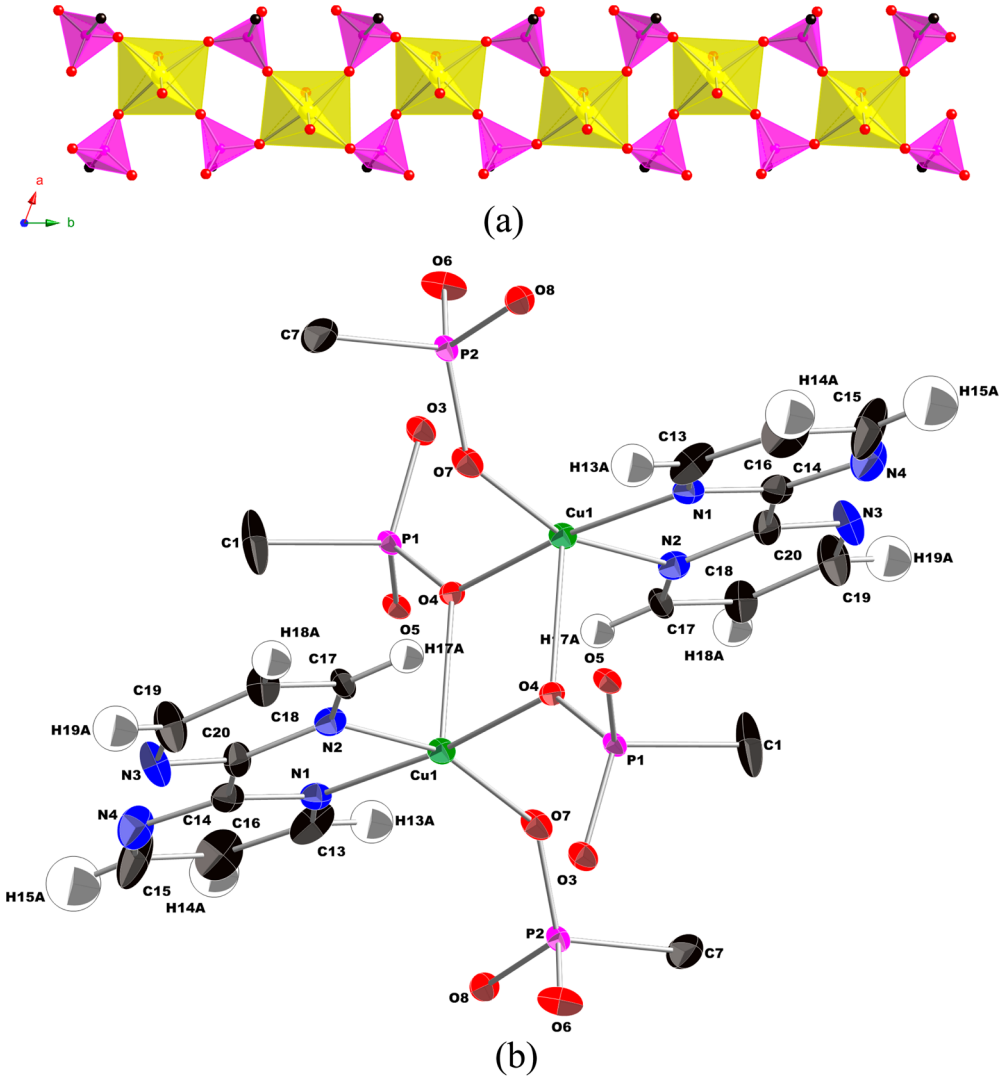

Figure 6. (a) A polyhedral representation of the uranyl-phosphonate chain in **3**, showing the UO_6 coordination environment. (b) A drawing of the local coordination environment in **3**, revealing the square pyramidal copper(II) dimer and the partially coordinated bipym linker. Ellipsoids are shown in the 50% probability level. [Legend is the same as that given in the caption for Figure 5.]

The Cu^{2+} center exhibits a distorted CuN_2O_4 (4 + 1 + 1) octahedral geometry.

Each uranium center is part of a UO_2^{2+} cation, with an average U═O bond distance of 1.769(5) Å. Four additional oxygen atoms from two phosphonate ligands coordinate the uranium cation in the equatorial plane, with U−O bond distances ranging from 2.235(5) Å to 2.343(5) Å. The calculated bond-valence sums at the uranium sites are 6.04 and 5.90 valence units, as expected for U^{6+}.[13] The P−O bond distances range from 1.499(5) Å to 1.596(5) Å and P−OH bond distances are much longer than P−O bond distances. The P(3)—O(12) {1.596(5)} and P(4)—O(14) {1.572(5)} bond distances are the longest P−O bonds; these O atoms are protonated and are the terminal oxygen atoms of the phosphonate groups. Two oxygen atoms from the PO_3 moieties and one chelating bipym coordinate to the copper center in the equatorial plane. The two coordination sites along the axial direction of the (4 + 1 + 1) octahedron are occupied by one oxygen atom from the phosphonate ligand and a co-crystallized water molecule, as shown in Figure 4b. The axial Cu−$O_{phosphonate}$ bond distance {2.669(6) Å} is much longer than the other Cu−O/N distances, but remains within the values in the literature.[14b] The second axial Cu−O_{water} bond distance {2.198(6) Å} is longer than the four equatorial Cu−O {1.902(5) Å and 2.025(5) Å} and Cu−N {2.045(6) Å and 2.052(6) Å} bond distances. The calculated bond valence sum for Cu(1) is 1.80, in agreement with the assigned oxidation state of Cu^{2+}.[13]

*Structure of Cu{(UO$_2$)(C$_6$H$_4$PO$_3$)$_2$(bipym)}·H$_2$O (**3**).* The overall structure of **3** contains one crystallographically distinct U^{6+} cation, one Cu^{2+} center that is partially chelated by bipym, and two phosphonate moieties (Figure 5). The coordination environment around the uranium center consists again of a relatively rare UO_6 tetragonal bipyramid (Figure 6a). The uranyl cations are arranged in a layer, and are linked into a pillared network by the diphosphonate ligands. One of the two ligands is canted with respect to the plane of the other ligand. The local coordination environment around the Cu^{2+} center is conspicuously distinct from those of the Cu^{2+} sites in **1** and **2**. The copper center is in a distorted five-coordinate CuN_2O_3 (4 + 1) square pyramidal geometry. The two phosphonate groups bridge the Cu^{2+} center to a symmetry-related Cu^{2+} site, resulting in a dimer (see Figure 6b).

The U^{6+} cation is coordinated to two nearly linear oxo atoms with an average U═O bond distance of 1.779(6) Å.

dx.doi.org/10.1021/ic500220d | Inorg. Chem. 2014, 53, 4169−4176

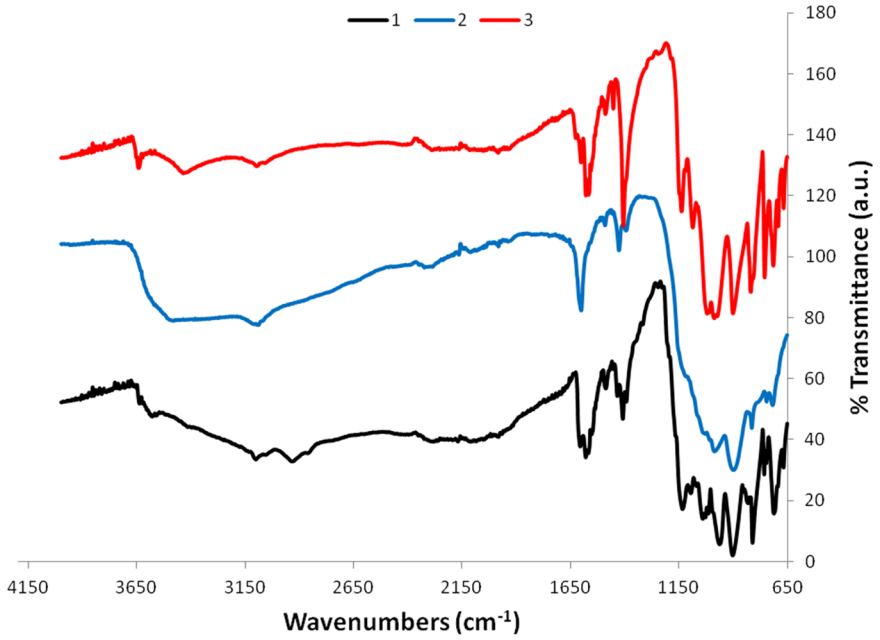

Figure 7. Infrared spectra of the three multidimensional polymetallic uranyl diphosphonate complexes (**1**, **2**, and **3**).

Four O atoms from the phosphonate groups are arranged in the equatorial plane with U−O bond distances that range from 2.266(5) Å to 2.294(5) Å. These bond distances give a bond-valence sum of 5.95 valence units for the uranium cation, which agrees with the assigned oxidation state of U^{6+}.[13] The P−O bond distances range from 1.514(6) Å to 1.541(6) Å; all are involved in the coordination to UO_2^{2+}/Cu^{2+} centers, so they are not protonated. The four equatorial positions of the Cu^{2+} square pyramid are occupied by two N atoms of the bipym and two O atoms of the phosphonate moiety, whereas the axial position is filled by an O atom of the phosphonate moiety. The Cu−O and Cu−N bond distances along the equatorial plane are {1.951(5) Å and 1.955(6) Å} and {1.999(7) Å and 2.042(7) Å}, respectively; these values are close to those found in compounds **1** and **2**. The $Cu(1)—O(4iii)_{axial}$ bond distance of 2.269(5) Å is much longer than the equatorial metal−ligand distances. The bond valence sum calculation for copper site is 1.82 valence units; this agrees with the Cu^{2+} oxidation state.[13]

Spectroscopic Properties. The absorption and fluorescence spectra are reported in the Figures S3 and S4 in the Supporting Information. The comprehensive description and peak assignments for the absorption and fluorescence spectra are given in our earlier work.[1b,c] The spectra for compounds **1** and **3** are red-shifted by 35 nm, whereas that of compound **2** is red-shifted by 102 nm, relative to the five-band emission pattern in the spectrum of $UO_2(NO_3)_2·6H_2O$. The differences between the spectra of these three compounds and $UO_2(NO_3)_2·6H_2O$ is due to the disparity in the coordination environment about the uranium cations. The infrared modes in the low wavenumber regions between 660 and 760 cm^{-1} (see Figure 7) consist of peaks indicative of O−P−O bending, phenyl ring, and P−C stretching vibrations. IR peaks ranging from 810 cm^{-1} to 990 cm^{-1} are attributed to the asymmetric and symmetric stretching modes of the uranyl cation. Those bands at 1014−1133 cm^{-1} in **1**, 1029 cm^{-1} in **2**, and 1010−1137 cm^{-1} in **3** are assigned to the symmetric and asymmetric stretching modes of phosphonates. The C−H bending of the phenyl ring is observed at 1434−1487 cm^{-1} for **1**, 1426 cm^{-1} for **2**, and 1452−1489 cm^{-1} for **3**. The sharp intense peaks at ∼1556−1598 cm^{-1} are the characteristic stretching modes of the bipym rings.[14a,b] The broad band near 1600 cm^{-1} is indicative of H_2O bending. The high-energy regions at ∼3500 cm^{-1} are usually dominated by the O−H stretches of the lattice water and Cu(II)-coordinated water.[1b,c,4a,11e]

CONCLUSIONS

The present work demonstrates a new strategy to build multidimensional polymetallic uranyl diphosphonate complexes by using bipym as a secondary linker. Importantly, the bipym group stabilizes the Cu^{2+} ions without truncating the dimensionality of the structure. Intriguingly, the elliptical cross-section of the nanotubular subunits and the dimension of the tubes in compounds **1** and **2** are similar to what we previously reported in $A_2\{(UO_2)_2F(PO_3HC_6H_4C_6H_4PO_3H)(PO_3HC_6H_4C_6H_4PO_3)\}·2H_2O$ (where A = Cs^+ and Rb^+).[5a] This result is significant because most of the design of polymetallic actinide complexes with auxiliary ligands (i.e., bidentate chelating ligands) yielded uranyl complexes with reduced dimensionality.[4] Moreover, this strategy could have wide synthetic utility in inorganic chemistry, opening up opportunities for the design of material with interesting topologies, physicochemical, and electronic properties.

ASSOCIATED CONTENT

Supporting Information

Selected interatomic distances (Å) and angles (deg), powder X-ray diffraction patterns, absorption and fluorescence spectra of three polymetallic uranyl diphosphonates (PDF). Crystallographic data of three polymetallic uranyl diphosphonates (CIF). This material is available free of charge via the Internet at http://pubs.acs.org.

AUTHOR INFORMATION

Corresponding Author

*E-mail: pburns@nd.edu.

Notes

The authors declare no competing financial interest.

dx.doi.org/10.1021/ic500220d | Inorg. Chem. 2014, 53, 4169−4176

■ ACKNOWLEDGMENTS

This material is supported by the Chemical Sciences, Geosciences and Biosciences Division, Office of Basic Energy Sciences, Office of Science, U.S. Department of Energy (Grant No. DE-FG02-07ER15880).

■ REFERENCES

(1) (a) Knope, K. E.; de Lill, D. T.; Rowland, C. E.; Cantos, P. M.; de Bettencourt-Dias, A.; Cahill, C. L. *Inorg. Chem.* **2012**, *51*, 201. (b) Adelani, P. O.; Oliver, A. G.; Albrecht-Schmitt, T. *Inorg. Chem.* **2012**, *51*, 4885. (c) Adelani, P. O.; Albrecht-Schmitt, T. *Cryst. Growth Des.* **2011**, *11*, 4676. (d) Adelani, P. O.; Oliver, A. G.; Albrecht-Schmitt, T. E. *Cryst. Growth Des.* **2011**, *11*, 3072. (e) Alsobrook, A. N.; Alekseev, E. V.; Depmeier, W.; Albrecht-Schmitt, T. *Cryst. Growth Des.* **2011**, *11*, 2358. (f) Alsobrook, A. N.; Hauser, B. G.; Hupp, J. T.; Alekseev, E. V.; Depmeier, W.; Albrecht-Schmitt, T. *Cryst. Growth Des.* **2011**, *11*, 1385. (g) Alsobrook, A. N.; Hauser, B. G.; Hupp, J. T.; Alekseev, E. V.; Depmeier, W.; Albrecht-Schmitt, T. E. *Chem. Commun. (Cambridge, U.K.)* **2010**, *46*, 9167. (h) Knope, K. E.; Cahill, C. L. *Eur. J. Inorg. Chem.* **2010**, 1177. (i) Alsobrook, A. N.; Zhan, W.; Albrecht-Schmitt, T. E. *Inorg. Chem.* **2008**, *47*, 5177.

(2) (a) Nelson, A. D.; Albrecht-Schmitt, T. E. *C. R. Chim.* **2010**, *13*, 755. (b) Nelson, A. D.; Bray, T. H.; Stanley, F. A.; Albrecht-Schmitt, T. E. *Inorg. Chem.* **2009**, *48*, 4530. (c) Nelson, A. D.; Bray, T. H.; Albrecht-Schmitt, T. E. *Angew. Chem., Int. Ed.* **2008**, *47*, 6252. (d) Diwu, J.; Wang, S.; Good, J. J.; DiStefano, V. H.; Albrecht-Schmitt, T. *Inorg. Chem.* **2011**, *50*, 4842.

(3) Tian, T.; Yang, W.; Wang, H.; Dang, S.; Sun, Z. *Inorg. Chem.* **2013**, *52*, 8288.

(4) (a) Yang, W.; Tian, T.; Wu, H.; Pan, Q.; Dang, S.; Sun, Z. *Inorg. Chem.* **2013**, *52*, 2736. (b) Wu, H.; Yang, W.; Sun, Z. *Cryst. Growth Des.* **2012**, *12*, 4669.

(5) (a) Adelani, P. O.; Albrecht-Schmitt, T. *Inorg. Chem.* **2011**, *50*, 12184. (b) Adelani, P. O.; Albrecht-Schmitt, T. E. *Angew. Chem., Int. Ed. Engl.* **2010**, *49*, 8909. (c) Shvareva, T. Y.; Almond, P. M.; Albrecht-Schmitt, T. E. *J. Solid State Chem.* **2005**, *178*, 499. (d) Shvareva, T. Y.; Sullens, T. A.; Shehee, T. C.; Albrecht-Schmitt, T. E. *Inorg. Chem.* **2005**, *44*, 300. (e) Shvareva, T. Y.; Skanthkumar, S.; Soderholm, L.; Clearfield, A.; Albrecht-Schmitt, T. E. *Chem. Mater.* **2007**, *19*, 132. (f) Ok, K. M.; Baek, J.; Halasyamani, P. S.; O'Hare, D. *Inorg. Chem.* **2006**, *45*, 10207.

(6) (a) Grohol, D.; Blinn, E. L. *Inorg. Chem.* **1997**, *36*, 3422. (b) Pozas-Tormo, R.; Moreno-Real, L.; Martinez-Lara, M.; Rodriguez-Castellon, E. *Can. J. Chem.* **1986**, *64*, 35. (c) Dorhout, P. K.; Rosenthal, G. L.; Ellis, A. B. *Solid State Ionics* **1989**, *32*−*33* (Part 1), 50.

(7) (a) S. Obbade, S.; Duvieubourg, L.; Dion, C.; Abraham, F. *J. Solid State Chem.* **2007**, *180*, 866. (b) Obbade, S.; Dion, C.; Saadi, M.; Abraham, F. *J. Solid State Chem.* **2004**, *177*, 1567. (c) Johnson, C. H.; Shilton, M. G.; Howe, A. T. *J. Solid State Chem.* **1981**, *37*, 37.

(8) Sykora, R. E.; Albrecht-Schmitt, T. E. *Inorg. Chem.* **2003**, *47*, 2179.

(9) (a) Yeon, J.; Smith, M. D.; Sefat, A. S.; zur Loye, H. *Inorg. Chem.* **2013**, *52*, 2199. (b) Mougel, V.; Chatelain, L.; Pécaut, J.; Caciuffo, R.; Colineau, E.; Griveau, J.; Mazzanti, M. *Nat. Chem.* **2012**, *4*, 1011. (c) Rinehart, J. D.; Harris, T. D.; Kozimor, S. A.; Bartlett, B. M.; Long, J. R. *Inorg. Chem.* **2009**, *48*, 3382. (d) Kozimor, S. A.; Bartlett, B. M.; Rinehart, J. D.; Long, J. R. *J. Am. Chem. Soc.* **2007**, *129*, 10672. (e) Mörtl, K. P.; Sutter, J.; Golhen, S.; Ouahab, L.; Kahn, O. *Inorg. Chem.* **2000**, *39*, 1626.

(10) (a) Thuery, P. *Inorg. Chem.* **2013**, *52*, 435. (b) Thuery, P.; Riviere, E. *Dalton Trans.* **2013**, *42*, 10551.

(11) (a) Adelani, P. O.; Albrecht-Schmitt, T. *Cryst. Growth Des.* **2012**, *12*, 5800. (b) Adelani, P. O.; Albrecht-Schmitt, T. E. *J. Solid State Chem.* **2012**, *192*, 377. (c) Adelani, P. O.; Albrecht-Schmitt, T. E. *J. Solid State Chem.* **2011**, *184*, 2368. (d) Adelani, P. O.; Oliver, A. G.; Albrecht-Schmitt, T. *Cryst. Growth Des.* **2011**, *11*, 1966. (e) Adelani, P. O.; Albrecht-Schmitt, T. *Cryst. Growth Des.* **2011**, *11*, 4227. (f) Adelani, P. O.; Albrecht-Schmitt, T. *Inorg. Chem.* **2009**, *48*, 2732.

(12) Sheldrick, G. M. *Acta Crystallogr., Sect. A: Cryst. Phys. Diffr., Theor. Gen. Crystallogr.* **2008**, *A64*, 211.

(13) (a) Burns, P. C.; Ewing, R. C.; Hawthorne, F. C. *Can. Mineral.* **1997**, *35*, 1551. (b) Brese, N. E.; O'Keeffe, M. *Acta Crystallogr., Sect. B: Struct. Sci.* **1991**, *B47*, 192.

(14) (a) Marino, N.; Armentano, D.; De Munno, G.; Cano, J.; Lloret, F.; Julve, M. *Inorg. Chem.* **2012**, *51*, 4323. (b) Demunno, G.; Julve, M.; Lloret, F.; Faus, J.; Verdaguer, M.; Caneschi, A. *Inorg. Chem.* **1995**, *34*, 157. (c) Demunno, G.; Julve, M.; Lloret, F.; Cano, J.; Caneschi, A. *Inorg. Chem.* **1995**, *34*, 2048. (d) Demunno, G.; Julve, M.; Nicolo, F.; Lloret, F.; Faus, J.; Ruiz, R.; Sinn, E. *Angew. Chem., Int. Ed. Engl.* **1993**, *32*, 613.